

Tracing the Evolution and Distribution of Metallicity in the Early Universe



Shelley A. Wright^{1,2}, David R. Law³, Richard S. Ellis⁴,
Dawn K. Erb⁵, James E. Larkin³, Jessica R. Lu⁴, Charles C. Steidel⁴

1 Center for Cosmology, UC Irvine, CA , 92697

2 saw@uci.edu ; (949) 824-0668

3 Department of Physics & Astronomy, UC Los Angeles, CA, 90095

4 California Institute of Technology, Pasadena, CA, 91125

5 Department of Physics, UC Santa Barbara, CA, 93106

Tracing the Evolution and Distribution of Metallicity in the Early Universe

Understanding metal enrichment over cosmic time is a core question in astrophysics. Metals are a fundamental parameter for cooling mechanisms in the intergalactic and interstellar medium, star formation, stellar physics, and planet formation. Heavy atomic nuclei trace the evolution of past and current stellar generations. Therefore, determining metallicities for individual galaxies, galactic substructures, and numerous galaxies over a range of redshifts will provide crucial constraints on galaxy formation. The upcoming decade offers promising prospects for expanding our knowledge of metal production in the young universe, and the mechanisms of their eventual dispersal into the galactic and extra-galactic environment.

1. Measuring metallicity evolution

To attempt to measure the evolution of metal enrichment, observers have used three primary techniques. First, in local galaxies ($\lesssim 10$ Mpc) where multiple stellar populations can be easily resolved, stellar archaeology has been used to try to piece together the history of metal production; however this is challenging, since present-day galaxies and galactic structures have had a significant amount of stellar mixing. Another method uses absorption lines in the neutral interstellar medium of damped Ly α (DLA) galaxies that fortuitously fall in our line-of-sight towards bright background quasars (Pettini et al. 2001; Kulkarni & Fall 2002; Prochaska et al. 2003). The third technique relies upon observation of rest-frame optical nebular emission lines from bright H II regions within actively star-forming galaxies. The relative strengths of these lines provide a diagnostic tool to identify both the abundance of heavy elements and the spectral shape of the ionizing flux distribution. While powerful, this method is observationally challenging since the surface brightness of galaxies fades dramatically as $(1+z)^4$ and (for redshifts $\gtrsim 1$) optical emission lines are redshifted into the near-infrared (NIR) where ground-based observations are hindered by higher atmospheric background. Only within the last decade, with the advent of more sensitive near infrared spectrographs and large collecting areas of 8-10m class telescopes has there been an attempt at specifically studying high redshift ($z \gtrsim 1$) galaxies using optical emission lines for metallicity diagnostics (Shapley et al. 2004, 2005; Savaglio et al. 2005; Erb et al. 2006; Maier et al. 2006; Liu et al. 2008; Maiolino et al. 2008).

A puzzling result of the high redshift studies is that metallicities derived from DLAs via UV absorption lines are an order of magnitude less than metallicities inferred from SFGs via optical emission lines. There are many explanations of this discrepancy. First, absorption line regions may be probing older, more pristine gas with lower metallicity that may lie in the outer regions of the host galaxies, whereas emission lines from star forming galaxies are tracing active H II regions with higher metallicity (Ellison et al. 2005). Another possibility is that at a given epoch DLAs and SFGs represent different galaxy populations with differing mass distributions and hence metallicities; however, this is difficult to assess as mass measurements of DLAs are currently unknown. Another consideration is that observed high redshift SFGs may be selected for achieving their peak star formation rate for their mass (Sandage et al. 2003; Noeske et al. 2007), whereas DLAs likely target a range of masses. Determining the cause of this discrepancy is one of

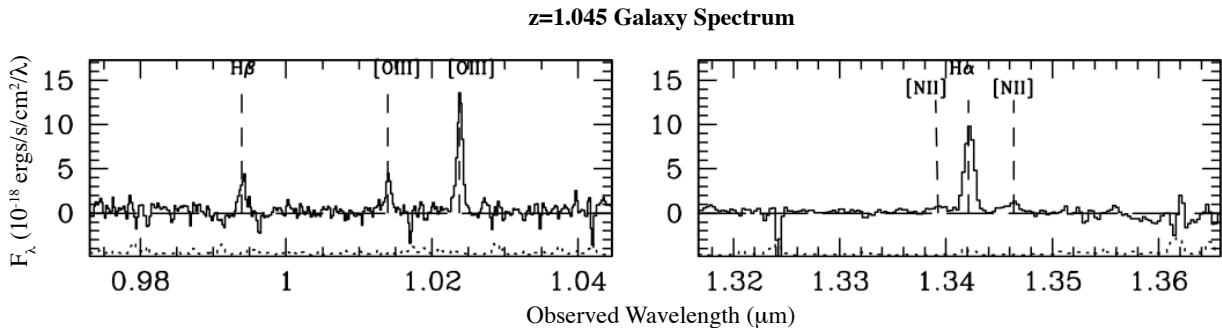


Fig. 1.— Example spectrum of $z = 1.045$ star forming galaxy from Shapley et al. (2005), using a single near-infrared long slit spectrograph on a 10m telescope. The spectrum shows typical emission lines ($H\beta$, $[O III]$, $H\alpha$, $[N II]$) that are used as chemical abundance diagnostics for high redshift systems ($z \gtrsim 1$).

the questions to pursue in this field in the coming decade.

2. Determining oxygen abundances in early star forming galaxies

Optical emission lines ($[O II]$, $H\beta$, $[O III]$, $H\alpha$, $[N II]$, $[S II]$) are traditionally used to empirically derive oxygen abundances of H II regions within the warm ISM of the Milky Way and local galaxies (Kewley et al. 2001, 2003, 2008, Ozbir et al. 2006). These empirical calibrations have been extended to high redshift galaxies (Pettini & Pagel 2004) for the brightest line ratio diagnostics ($[O III]/H\beta$ and $[N II]/H\alpha$). In Figure 1, an integrated spectrum of a star forming galaxy at $z=1.045$ is shown to illustrate line emissions used to derive chemical abundances. It has been observed that there is an offset between excitation levels seen in local star forming galaxies from that of the high redshift galaxy samples (Shapley et al. 2004, 2005; Savaglio et al. 2005; Erb et al. 2006; Liu et al. 2008). Emission lines are generated from different excitation mechanisms, which are based on the excitation energy, hardness of the ionizing spectrum, and chemical abundances. Traditional Baldwin et al. (1981; BPT) diagrams are used to distinguish between line emission that is either generated from H II regions in star forming galaxies or active galactic nuclei (AGN). Within this diagram there is an empirical trend among local star forming galaxies with a spread of metallicities, and a distinguishing spread of AGN, LINERS, and transitional objects. Figure 2 illustrates this local star forming galaxy distribution as seen from the SDSS survey. Over-plotted are the high redshift nebular ratios from Liu et al. 2008 ($z \sim 1.0$ and 1.4) and Erb et al. 2006 ($z \sim 2$), which are above the local relation. These results imply that at high redshift either star formation within H II regions is different (e.g., greater e^- densities compared to local H II regions), the IMF is different (e.g., harder ionizing spectrum), and/or these observations may have some AGN contamination which is elevating these values.

Metallicity studies typically target galaxies that have no signs of AGN activity, as seen from their SED (i.e., from HST and Spitzer imaging) and their rest-frame UV spectroscopy. However, possible evidence for weak AGN activity has recently been discovered within $z \sim 1.6$ galaxies seen with an integral field spectrograph coupled with an adaptive optics system (Wright et al. 2008).

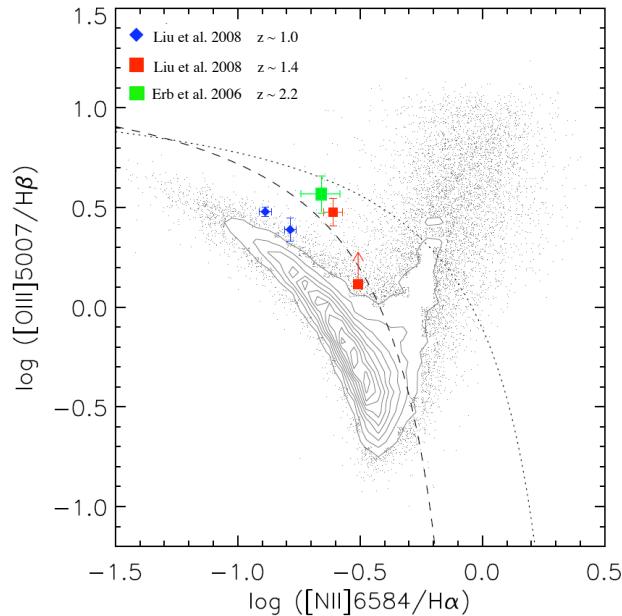


Fig. 2.— An optical emission line ratio plot of $\log([\text{O III}]/\text{H}\beta)$ versus $\log([\text{N II}]/\text{H}\alpha)$, as shown by Liu et al. 2008. This plot is typically used to distinguish between excitation mechanisms either generated from star forming galaxies or AGN. Small black points and contours represent the distribution of local galaxies ($z \sim 0.07$) within the Sloan Digital Sky Survey (SDSS) (Tremonti et al. 2004). The $z \sim 1.0$ (red) and $z \sim 1.4$ (blue) galaxies from Liu et al. 2008 and $z \sim 2.2$ (green) galaxies from Erb et al. 2006 are overplotted, illustrating that they lie above the local distribution of star forming galaxies. Star forming galaxies and H II regions are located in the tight, densely populated sequence to the left of the dashed curve line of the empirical limit of star forming galaxies based on the SDSS sample (Kauffmann et al. 2003). The dashed curve represents a theoretical limit from Kewley et al. (2001) based on models of star forming galaxies, LINERs and AGN lie up and to the right of the star forming galaxy distribution.

These galaxies have high $[\text{N II}]/\text{H}\alpha$ ratios concentrated into very small regions ($\lesssim 0''.1$). This is shown in Figure 3, where the ratio of $[\text{N II}]/\text{H}\alpha$ is mapped spatially across one of these galaxies. Without the high spatial resolution of adaptive optics and 2D mapping capabilities of integral field spectrographs, these weak AGN would not have been discovered since none of these galaxies have SEDs or UV spectra indicative of hosting an AGN. This poses an interesting conundrum of whether our current understanding of metallicity-evolution holds true, or whether at least some galaxies used in current metallicity studies were contaminated by underlying AGN emission. In addition, high angular resolution integral field spectrograph observations present the possibility of mapping 2D metallicity distributions across individual high redshift galaxies. This technique offers potential for discovering abundance differentials between galactic substructures, outflows, and inflows during prime epochs of galaxy assembly.

3. Tracing mass-metallicity evolution

The relationship between metallicity of a galaxy and its total stellar mass is well-known in the local universe (Lequeux 1979). Recently, this empirical mass-metallicity (MMZ) relationship

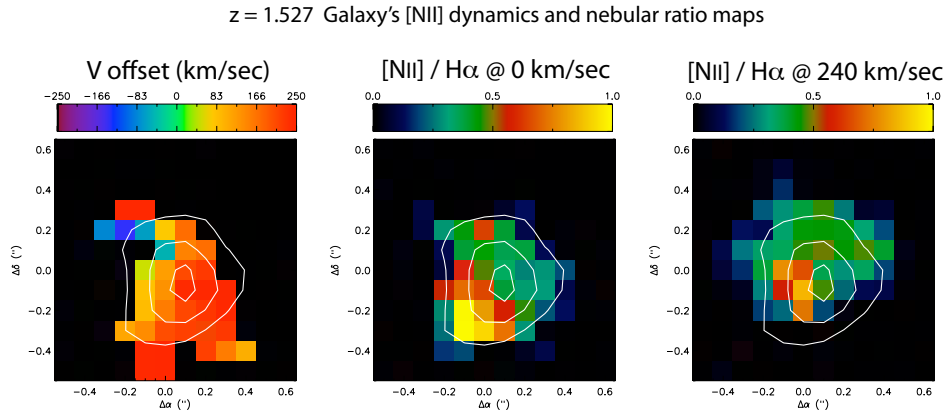


Fig. 3.— Two-dimensional metallicity maps of a star forming galaxy at $z = 1.53$ are presented from Wright et al. (2008), which used integral field spectrograph with laser guide star adaptive optics observations. $[N II]/H\alpha$ ratio maps illustrate locations of high and low nebular ratios at different velocity locations. Contours of $H\alpha$ emission is overplotted on each image. (LEFT) $[N II]$ velocity offsets with respect to the mean $H\alpha$ redshift for each source. (MIDDLE) Ratio of $[N II]/H\alpha$ at the peak location of $H\alpha$ emission (0 km s^{-1}). (RIGHT) Ratio of $[N II]/H\alpha$ at the peak location $[N II]$ emission at 240 km s^{-1} . There is a high $[N II]/H\alpha$ ratio concentrated in one to two spatial elements for each source, with lower $[N II]/H\alpha$ values occurring elsewhere within the galaxy. This implies there is a central AGN within this source, indicated by the locations of the high $[N II]/H\alpha$ locations, while the rest of the galaxy show smaller nebular ratios.

has been greatly enhanced with the large local ($z \lesssim 0.1$) galaxy sample from the Sloan Digital Sky Survey (SDSS; Tremonti et al. 2004), which shows that galaxies with higher stellar masses have higher metallicities. Multiple scenarios are proposed to explain the local MMZ relationship. A primary interpretation is that less massive galaxies with a smaller potential-well are more likely to lose their metals through galactic outflows (ie, from starburst winds and SNe) into the intergalactic medium, and therefore show less metal enrichment. Alternatively, low mass galaxies (which typically have large gas fractions) may be more metal-poor simply because they have not yet converted the majority of their gas into stars, while the bulk of star formation in more massive galaxies may have occurred at higher redshift. Characterizing the MMZ relationship at high redshift therefore allows a powerful means for constraining galaxy formation and evolution.

Extending the local MMZ relationship to higher redshift has been attempted by some authors using optical nebular ratios as described above (Savaglio et al. 2005; Erb et al. 2006; Liu et al. 2008; Maiolino et al. 2008). In Figure 4, Maiolino et al. (2008) present a comparison of the observed MMZ relationships from different samples and redshift regimes ($z = 0.07, 0.7, 2.2,$ and 3.5). The MMZ relationship shows some evolution between these regimes; namely, galaxies of a given stellar mass tend to be more metal poor at high redshifts than in the local universe. There have only been a handful of studies at high redshift, and better constraining the overall shape of the MMZ relationship at any given cosmic epoch and the overall evolutionary trend is imperative for our understanding of metal enrichment and galaxy formation.

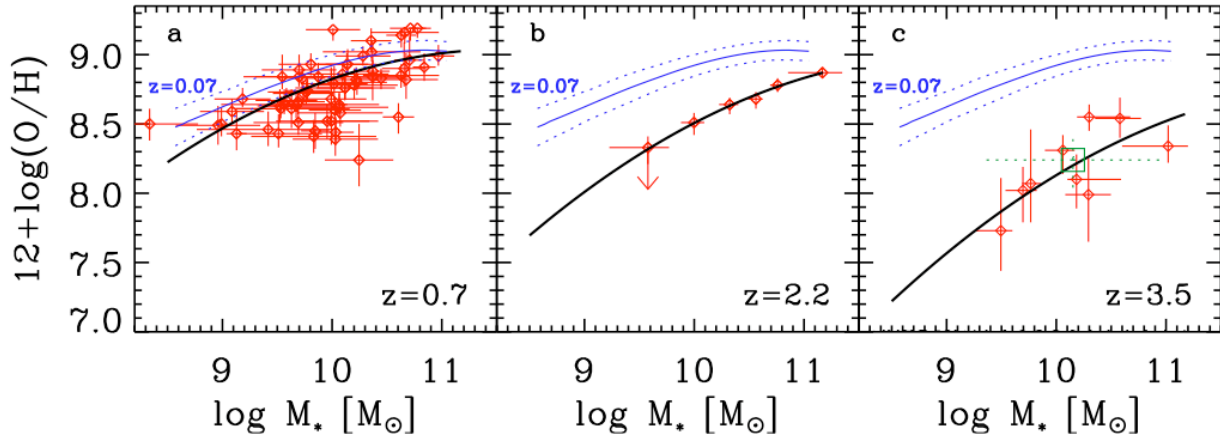


Fig. 4.— *The mass-metallicity relation observed at varying redshift bins relating oxygen abundance and stellar mass of the host galaxy, presented in Maiolino et al. (2008). These redshift regimes have been observed with differing studies, where $z=0.07$, $z=0.7$, $z=2.2$, and $z=3.5$ measurements (red points) are from Kewley & Ellison (2008), Savaglio et al. (2005), Erb et al. (2006), and Maiolino et al. (2008), respectively. The blue solid and dotted lines represent the observed dispersion at $z=0.07$ (Kewley & Ellison 2008). Each black curve has been parameterized by an analytic function at each redshift bin with the best fit parameters to the observed stellar masses and oxygen abundances.*

4. Questions for the next decade

Within the last decade we have made significant progress toward understanding chemical abundances at high redshift and the MMZ evolutionary trend, but these discoveries have generated a rich set of questions for understanding the production of metals over cosmic time and how that relates to galaxy formation. We outline a few of these questions that will potentially be answered by missions and instruments planned for the coming decade:

1) Does the MMZ relationship hold for lower mass galaxies ($M_* \lesssim 10^{10} M_\odot$) at high redshift? How does this relation evolve beyond $z \sim 3$?

2) How do galaxies exchange metals into the IGM? Does mass loss through outflows in less massive galaxies contribute to the origin of the MMZ relationship at high redshift?

3) What are the two-dimensional metallicity gradients in high redshift galaxies? Are there metallicity differentials within early substructures (e.g, bulges, merger components, outflows)?

4) How does metallicity vary for different types of morphologically/dynamically distinct high redshift galaxies? How do accretion and merging affect metallicity of an individual galaxy?

5) What is the origin of the heightened excitation values from nebular ratios found at high redshift compared to local galaxies (Figure 2)? Are these elevated nebular ratios caused by different physical conditions in H II regions, a different IMF at high redshift, or from AGN activity?

6) What is the origin of the apparent metallicity differential between absorption line DLAs and emission line star forming galaxies? Are these different populations of galaxies, or is the differential caused by probing different environmental regions?

5. Technical aspects

The preceding questions are some of the major science drivers for future telescopes and instruments, such as the James Webb Space Telescope (JWST), extremely large ($\sim 30\text{m}$) ground-based telescopes (ELTs), near-infrared multi-object spectrographs, and new high angular resolution techniques using adaptive optics (AO) on 8-10m class telescopes and ELTs.

5.1. Generating a significant sample across redshift

One of the major barriers to answering these questions are the statistically small numbers of galaxies currently observed at high redshift. For instance, our current picture of the MMZ relationship relies on a sample of a mere 10 to 20 galaxies in only a few redshift bins beyond $z \sim 1$. It is clear that much larger statistical samples are needed at a range of redshifts.

Multi-object spectrographs offer the best means to develop these samples, and several missions are currently being developed with the potential to do this work. There are seeing-limited multi-object spectrographs (~ 40 objects per observation) scheduled to come online in the next few years on 8 and 10m telescopes that will generate a significant catalog of rest-frame optical spectra ($1 \lesssim z \lesssim 3$) for bright star forming galaxies. JWST and ELT missions are also proposing multi-object spectrographs that will have unprecedented sensitivity, and will extend these observations both to fainter ($\lesssim 1 M_{\odot} \text{ yr}^{-1}$), lower-mass star forming galaxies and to higher redshifts ($1 \lesssim z \lesssim 6$). Both JWST and ELTs are complementary with each having unique strengths. ELT multi-object spectrographs will have a factor of 3 times greater spectral resolution than JWST's multi-object spectrograph, yielding a higher velocity resolution that may be coupled with spatially unique abundance regions. JWST will have better sensitivity at longer infrared wavelengths ($\gtrsim 1.8 \mu\text{m}$), where certain prime emission lines are redshifted (e.g., $\text{H}\alpha$, $[\text{O III}]$ emission from $z = 2, 3$), but ELTs and JWST will have comparable sensitivity at shorter infrared wavelengths. All of these measurements will push well beyond our current observations and go deeper into the early universe.

5.2. Identifying substructures and flows from 2D metallicity maps

The advent of near-infrared integral field spectrographs coupled with adaptive optics adds a new, intimate view of galaxy chemo-dynamical properties across a two dimensional area with sub-kiloparsec resolutions (Genzel et al. 2006, 2008; Law et al. 2007, 2009; Wright et al. 2007, 2008). These studies have been able to measure the brightest $\text{H}\alpha$ emission from high redshift galaxies, but in only a few cases are weaker lines ($\text{H}\beta$, $[\text{O III}]$, and $[\text{N II}]$) reached with current sensitivity limits. With upcoming integral field spectrographs on ELTs and JWST, observations will be able to probe emission lines, with a factor of 10 - 100 sensitivity gain over current 8-10m facilities. Adaptive optics on ELTs will yield superb spatial resolutions with a factor of 3 angular resolution gain over current capabilities, and will be able to dissect high redshift galactic structures. For instance, an integral field spectrograph on an ELT with adaptive optics will be able to map $\text{H}\alpha$ emission for a galaxy at $z = 2$, with a star formation rate $\lesssim 0.1 M_{\odot} \text{ yr}^{-1}$ spread over an arcsecond. At these spatial scales, high redshift galaxies will be spectrally mapped to 50-100 pc resolutions, probing the star formation history and abundances of large H II regions and individual super star clusters. This

will offer the ability to compare the metallicity of different components of high redshift galaxies, such as differentiating abundances between a central bulge versus the more extended outer regions of the galaxy. In addition, coupling abundances with the dynamics of these galaxies will offer a method for distinguishing small mergers from outflows/inflows within individual galaxies. This will allow direct investigation of the metal enrichment of the intergalactic medium at each redshift range. ELTs and JWST will provide an unprecedented level of astrophysical detail for high redshift galaxies, and will offer new insight into the questions of metal production over cosmic time and galaxy formation.

REFERENCES

- Baldwin, J. A., Phillips, M. M., & Terlevich, R. 1981, *PASP*, 93, 5
- Ellison, S. L., Kewley, L. J., & Mallén-Ornelas, G. 2005, *MNRAS*, 357, 354
- Erb, D. K., Shapley, A. E., Pettini, M., Steidel, C. C., Reddy, N. A., & Adelberger, K. L. 2006, *ApJ*, 644, 813
- Genzel, R., et al. 2006, *Nature*, 442, 786
- Genzel, R., et al. 2008, *ApJ*, 687, 59
- Kauffmann, G., et al. 2003, *MNRAS*, 346, 1055
- Kewley, L. J., Dopita, M. A., Sutherland, R. S., Heisler, C. A., & Trevena, J. 2001, *ApJ*, 556, 121
- Kewley, L. J., & Ellison, S. L. 2008, *ApJ*, 681, 1183
- Kulkarni, V. P., & Fall, S. M. 2002, *ApJ*, 580, 732
- Maier, C., Lilly, S. J., Carollo, C. M., Meisenheimer, K., Hippelein, H., & Stockton, A. 2006, *ApJ*, 639, 858
- Maiolino, R., et al. 2008, *A&A*, 488, 463
- Law, D. R., Steidel, C. C., Erb, D. K., Larkin, J. E., Pettini, M., Shapley, A. E., & Wright, S. A. 2007, *ApJ*, 669, 929
- Law, D. R., Steidel, C. C., Erb, D. K., Larkin, J. E., Pettini, M., Shapley, A. E., & Wright, S. A. 2009, arXiv:0901.2930
- Lequeux, J. 1979, *A&A*, 80, 35
- Liu, X., Shapley, A. E., Coil, A. L., Brinchmann, J., & Ma, C.-P. 2008, *ApJ*, 678, 758
- Noeske, K. G., et al. 2007, *ApJ*, 660, L43
- Pazder, J. S., Roberts, S., Abraham, R., Anthony, A., Fletcher, M., Hardy, T., Loop, D., & Sun, S. 2006, *Proc. SPIE*, 6269,
- Pettini, M., Ellison, S. L., Schaye, J., Songaila, A., Steidel, C. C., & Ferrara, A. 2001, *Astrophysics and Space Science Supplement*, 277, 555
- Pettini, M., & Pagel, B. E. J. 2004, *MNRAS*, 348, L59
- Posselt, W., Holota, W., Kulinyak, E., Kling, G., Kutscheid, T., Le Fevre, O., Prieto, E., & Ferruit, P. 2004, *Proc. SPIE*, 5487, 688
- Prochaska, J. X., Gawiser, E., Wolfe, A. M., Castro, S., & Djorgovski, S. G. 2003, *ApJ*, 595, L9
- Sandage, A., Lubin, L. M., & Vandenberg, D. A. 2003, *PASP*, 115, 1187
- Savaglio, S., et al. 2005, *ApJ*, 635, 260
- Shapley, A. E., Erb, D. K., Pettini, M., Steidel, C. C., & Adelberger, K. L. 2004, *ApJ*, 612, 108
- Shapley, A. E., Coil, A. L., Ma, C.-P., & Bundy, K. 2005, *ApJ*, 635, 1006
- Tremonti, C. A., et al. 2004, *ApJ*, 613, 898
- Wright, S. A., et al. 2007, *ApJ*, 658, 78
- Wright, S. A., Larkin, J. E., Law, D. R., Steidel, C. C., Shapley, A. E., & Erb, D. K. 2008, arXiv:0810.5599